

RESEARCH ARTICLE

Plant Mediated Synthesis of ZnO Nanoparticles Using *Butea monosperma* Plant Extract and Their Antibacterial Applications

Tanika Thakur¹, Manish Kumar², Abhishek Walia³, Deepika Kaushal^{1,*}

ABSTRACT: Plant based nanoparticles (NPs) has become an emerging field in nanotechnology in terms of cost efficiency, less hazardous, biocompatibility and ecologically benignancy. Further, These NPs are being extensively studied for their use as nanomedicines and novel antibacterial agents due to increased growth of hazardous bacteria and their increased resistance to traditional antibiotics. The present studies focused on biosynthesis of zinc oxide (ZnO) NPs using the chloride derivative of zinc and aqueous extract of *Butea monosperma* (BM) plant and its antibacterial applications on food borne pathogens. Scanning electron microscopy (SEM) reveals the formation of mixed shaped (spherical and hexagonal) ZnO NPs with size ranging between 20-90 nm. The elemental composition of various constituents present in the resulting samples was confirmed from energy dispersive X-ray (EDX). XRD pattern suggested crystalline nature with hexagonal wurtzite structure of ZnO NPs. The Scherrer formula is used to evaluate the average crystallite size of the synthesized NPs ranges from 15 to 85 nm. Furthermore, the Tauc plot method was employed to determine the bandgap energies of the biosynthesized ZnO NPs using UV-visible spectra. These NPs were found to be effective against bacterial strains; *Staphylococcus aureus* (MTCC 96), *Bacillus cereus* (MTCC 1272), *Stenotrophomonas maltophilia* (MTCC 4383), *Shigella flexneri* (MTCC 1457). Overall, this present research describes that synthesized ZnO NPs hold significant importance as potential antibacterial agents against gram positive bacteria.

Keywords: *Butea monosperma*, zinc oxide nanoparticles, synthesis, antibacterial, pathogens

Received: 23 March 2024; Revised: 28 April 2024; Accepted: 07 June 2024; Published Online: 17 July, 2024

1. INTRODUCTION

Nanotechnology is revolutionary field flourished with nanoparticles having size ranges from 1-100 nm in at least one dimension that are used extensively in all fields [1, 2]. The nano size generally refers to large surface area that significantly different from bulk materials. The increased surface area to volume ratio as well as increased reactivity on

the surface are responsible for unique physical, chemical and antibacterial properties of nanoscale materials [3, 4]. These properties make nanomaterials useful in area of energy, medicine, electronics, sensors and environment [5]. A variety of physical, chemical and biological methods are available for the synthesis of these nanoparticles. Among all, physical and chemical methods have hazardous effects on human health whereas biological methods have no such harmful effects as no toxic chemicals are used during synthesis [6]. Synthesis via biological methods include various entities like plants, bacteria, fungi and algae [7]. Plant extract-based synthesis is one of the safest, economical, non-hazardous and large-scale synthesis method and nanoparticles formed in this way are much stable in comparison to those produced by other microorganisms [8, 9]. Plant extracts contain a variety of active biomolecules and phytochemicals that are responsible for the stability of nanoparticles [10, 11].

Numerous metals are used for the plant-based synthesis

¹ Department of Chemistry, Sri Sai University, Palampur, Kangra-176081, Himachal Pradesh, India.

² Department of Chemistry & Chemical Sciences, Central University of Himachal Pradesh, Dharamshala, Kangra-176206, Himachal Pradesh, India.

³ Department of Microbiology, Chaudhary Sarwan Kumar Himachal Pradesh Agricultural University, Palampur-176062, Himachal Pradesh, India.

* Author to whom correspondence should be addressed:
dkaushal28@gmail.com (Deepika Kaushal)

of nanoparticles but most of the metals are toxic and causes numerous side effects to living organisms which make these materials unfit for medical industry [12]. Out of various nanoparticles, ZnO NPs have engrossed all the attention of many researchers in the field of cosmetic, environmental safety and medicinal industries due to its non-toxic nature and broad band gap of 3.1 to 3.3 eV [13, 14]. ZnO is a n type semiconductor which shows good antimicrobial activity in comparison to other materials [15]. ZnO NPs have been prepared from variety of plant and fruit extracts such as *Passiflora caerulea* [16], *Myristica fragrans* [17], *Azadirachta indica* [18], *Cinnamomum verum* [19], *Duranta erecta* [20], *Vitex trifolia* [21] *Matricaria chamomilla* L., *Lycopersicon esculentum* M. and *Olea europaea* [22] in which their antibacterial activities were also reported. Zinc oxide nanoparticles synthesized by green methods have multifunctional properties and dynamic antibacterial activity, as a result, there is a necessity for a simple and environmentally safe technique for ZnO NPs synthesis [23].

In today's scenario, bacterial infections pose serious threats to mankind, extending to social and economic problems. The increased resistance to antibiotics, emergence of infectious strains, development of new bacterial mutations, and deficiency of appropriate vaccines are critical health hazards. Thus, the discovery and development of novel antibacterial agents against common bacterial strains are imperative. In this context, zinc oxide nanoparticles (ZnO NPs) have shown remarkable antibacterial activity against various bacterial species, as discovered by researchers worldwide [24, 25]. ZnO is considered a useful antibacterial agent in both nano and microscale formulations. Particularly, when the particle size is reduced to the nano range, ZnO NPs exhibit enhanced antibacterial activities due to their ability to penetrate bacterial cell walls and disrupt cellular functions through distinct mechanisms [26, 27]. Moreover, plant-mediated ZnO NPs have demonstrated superior antibacterial activity compared to conventional ZnO NPs. This enhanced activity is likely due to the transfer of medicinal properties from the plants to the ZnO NPs during synthesis, which adds to their antibacterial efficacy. These properties make plant-mediated ZnO NPs a promising candidate for developing new antibacterial agents, addressing the urgent need for effective treatments against resistant bacterial strains and contributing to better healthcare outcomes.

In the present work, we have selected plant *Butea monosperma* (BM) for the preparation of ZnO NPs. BM is available in different parts of Asia including India, Japan, Indonesia, Nepal, Vietnam, Thailand and Sri Lanka. In India, it is widely distributed in various states including Himachal Pradesh, Jammu and Kashmir, Assam, Punjab, Kerala, Orissa and West Bengal [28]. The chosen plant has significant medicinal properties especially analgesic, aphrodisiac, anti-helminthic, anti-stress, antimicrobial, antioxidant, anticancer and antifertility properties. The plant is also used to cure many skin diseases as well as in diabetes.

The present study entitled "Plant mediated synthesis of ZnO Nanoparticles using *Butea monosperma* plant extract and their Antibacterial applications" involves biosynthesis of

ZnO NPs via BM plant, their characterization and their antibacterial activities against some foodborne pathogens.

2. EXPERIMENTAL DETAILS

All the materials viz. Zinc Chloride ($ZnCl_2$), Sodium hydroxide (NaOH) of analytical grade were procured from SRL Pvt. Ltd and MOLYCHEM and used as such without additional purification. Double deionized water was used to prepare all the samples.

2.1. Preparation of plant extract

The flower, leaves and bark of BM were collected from Nagrota Bagwan village of Kangra district, H.P. India. The plant was identified by Plant Taxonomy department of CSIR, Palampur (Reference number: PLP- 22015). The powdered form of plant materials was used for extract preparation. About 100 g of mixture powder mixed in 1000 mL deionized water was kept on water bath for boiling until the plant extract is reduced to 500 mL and the color of solution changes. The resultant mixture was filtered with "Whatman filter paper" to eliminate any undesirable residue. The final extract obtained was kept at 4 °C for future use. Figure 1 demonstrates the digital images of powdered form of *Butea monosperma* obtained from flower, leaves, and bark.

2.2. Synthesis of ZnO NPs

ZnO NPs were prepared by using two methods: without plant (ZnO) and with plant extract (BM-ZnO).

2.2.1. Synthesis of ZnO NPs (without Plant extract)

ZnO NPs were prepared by using 0.1M of $ZnCl_2$ solution which then kept on magnetic stirrer at temperature 50 °C. The reaction was maintained at basic pH by the dropwise addition of 0.1M NaOH solution with continuous stirring till the precipitation is complete. The color changes from colorless to white colored precipitates indicates the formation of ZnO NPs. The obtained precipitates were washed and kept in the oven at 100 °C temperature for two hours. The obtained sample was calcinated at 450 °C and 750 °C temperatures.

2.2.2. Synthesis of ZnO NPs (with Plant extract)

Firstly, 50 ml of plant extract solution was added on to 0.1M $ZnCl_2$ solution and stirred for about one hour in a magnetic stirrer. To maintain basic pH, 0.1M NaOH solution was also added with continuous stirring till the precipitation is complete. Appearance of pale yellow-colored precipitates confirmed the deposition of BM-ZnO NPs. The precipitates were allowed to settle overnight before filtration. After washing, the precipitates were kept in the oven at 100 °C temperature for two hours. The obtained sample was calcinated at 450 °C, and 750 °C temperatures.

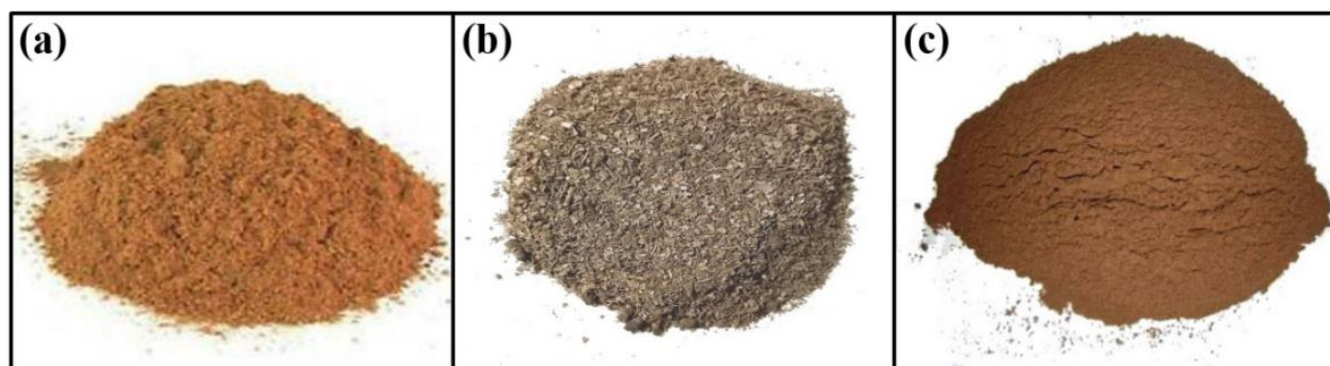


Fig. 1. Digital images of powdered form of *Butea monosperma*, obtained from (a) flower, (b) leaves, and (c) bark.

2.3. Characterization of ZnO NPs

To corroborate the efficacious synthesis, structural shape, size and morphology, the prepared NPs were examined and analyzed with variety of characterizations. The crystallinity of the sample and measurement of sample purity was identified by XRD [29]. Here, the crystalline structure and crystallite size of all prepared samples was analyzed using a Rigaku corporation Smart lab model having a 9kw rotating anode diffractometer. In order to measure the absorption spectra or optical density and band gap studies of synthesized nanoparticles, Shimadzu's UV-visible spectrophotometer model UV-2450 was used in the range between 180-800 nm. Similarly, Nova Nano SEM 450 analyzer with acceleration voltage 10 KV was used for SEM and EDX.

2.4. Antibacterial studies

The antibacterial applications of the synthesized ZnO NPs were assessed by standard "agar well diffusion method" against four different pathogenic strains: Gram-positive '*Bacillus cereus* (MTCC 1272), *Staphylococcus aureus* (MTCC 96)' and Gram-negative '*Stenotrophomonas maltophilia* (MTCC 4383) and *Shigella flexneri* (MTCC 1457)' [30]. All these studies have been carried out at Agriculture University CSKHPKV, Palampur. Before microbiological analysis, standard solutions of 1 mg ml⁻¹ concentrations were prepared in water and all solutions were filtered with microbiological filters with pore size of 0.2 µm. The Nutrient agar and broth were used for bacterial cultivation. Before performing the experiments, all bacteria were sub-cultured on media and incubated for 24 hours at a temperature of 35 ± 2 °C. Then suspensions of microorganisms were prepared and their density was maintained at 0.5 according to McFarland Standard, in densitometer. With the help of sterile cork borers, the suspensions of microorganisms overlaid with agar media were punched to create a well of 10 mm diameter, to which 100 µl of tested substances have been introduced. The plates were then incubated for 24 h at a temperature of 35 ± 2 °C depending on the indicator microorganism. The diameter of the inhibition zones was determined in millimeters after the

incubation time was completed. The tests were performed in triplicates with the results reported as mean values.

3. RESULTS AND DISCUSSION

3.1. XRD Analysis

The typical pattern of PXRD of bare ZnO NPs at different temperatures are shown in Figure 2 (a, b). XRD peaks of bare ZnO (450°C) are observed at $2\theta = 31.87^\circ, 34.53^\circ, 36.35^\circ, 47.63^\circ, 56.67^\circ, 62.95^\circ, 66.44^\circ, 68.02^\circ, \text{ and } 69.16^\circ$ values with lattice planes at (100), (002), (101), (102), (110) (103), (112) and (201), respectively. The peak intensity of all the samples is extremely high, indicating good crystalline formation. The most intense peak is attained at 36.35° shows the existence of hexagonal wurtzite phase. The Debye-Scherrer's equation was used to evaluate crystallite size which was found to be 50 nm with lattice strain 0.0023 [31, 32]. The peaks are well matched with standard ZnO (JCPDS36-1451) with lattice parameter $a=b=2.851, c=4.939\text{\AA}$ [33]. ZnO NPs at 750 °C also depicted the same pattern with crystallite size 82 nm and lattice strain of 0.0014. Increased crystallite size with calcination temperature indicates phase stability of ZnO NPs [34, 35]. Further, at higher temperature the increased surface energy responsible for grain boundary migration, which causes small grains to agglomerate and form large grains. The same findings have also been stated in previous studies [36].

Similarly, the PXRD pattern of BM-ZnO at both temperatures are shown in Figure 3 (a, b). The graph shows different peaks at 31.78°, 34.45°, 36.26°, 47.56°, 56.60°, 62.88°, 67.96°, and 69.08° with lattice planes at (100), (002), (101), (102), (110), (103), (201), (004), respectively. These values confirm the phase of ZnO NPs as hexagonal wurtzite [37]. The calculated crystallite size was 18 nm with lattice strain of 0.0061. ZnO NPs at 750 °C also depicted the same pattern with peaks at 31.83°, 34.49°, 36.31°, 47.61°, 56.66°, 62.94°, 68.02° and 69.15° having crystallite size 27 nm with lattice strain 0.0043. The increase in the sharpness of XRD peaks and decrease in FWHM with rise in temperatures, indicates the dominance of crystalline nature as calcination

temperature rises [38].

Further, the advantage of plant extracts is to reduce ions and confined the nanoparticles to inhibit their growth into large particles [39]. In view of above fact, on comparison of bare and BM-ZnO NPs, it is found that intensity of BM-ZnO NPs decreases due to the influence of plant extract in the bio-reduction of ZnO NPs.

The incorporation of plant's organic constituents in crystal lattice causes strain in lattice which decreases the crystallinity. This is further supported by the reduction in crystallite size of BM-ZnO relative to bare ZnO at both temperatures [40]. The values of crystallite size, lattice strain and lattice parameters for bare ZnO and BM-ZnO at 450 °C and 750 °C have been reported in Table 1.

3.2. Scanning Electron microscopy and EDX studies

The grain size and morphological structure of biosynthesized ZnO NPs were determined using SEM analysis. Figure 4 (a, b) shows a SEM image of BM-ZnO NPs which indicates individual ZnO particle as well as aggregation of particles. The shapes of nanoparticles are mostly spherical and hexagonal with particle sizes between 20 to 90 nm [41].

The composition of various elements contained in BM-ZnO nanoparticles is depicted in the EDX spectrum (Figure 4(c)). The appearance of Zn and O peaks with weight percentages of 79.28 and 14.98 is confirmed by EDX spectra. Carbon and nitrogen elemental peaks were also found with weight percentages of 2.96 and 2.78 respectively owing to the presence of these elements in the *BM* plant.

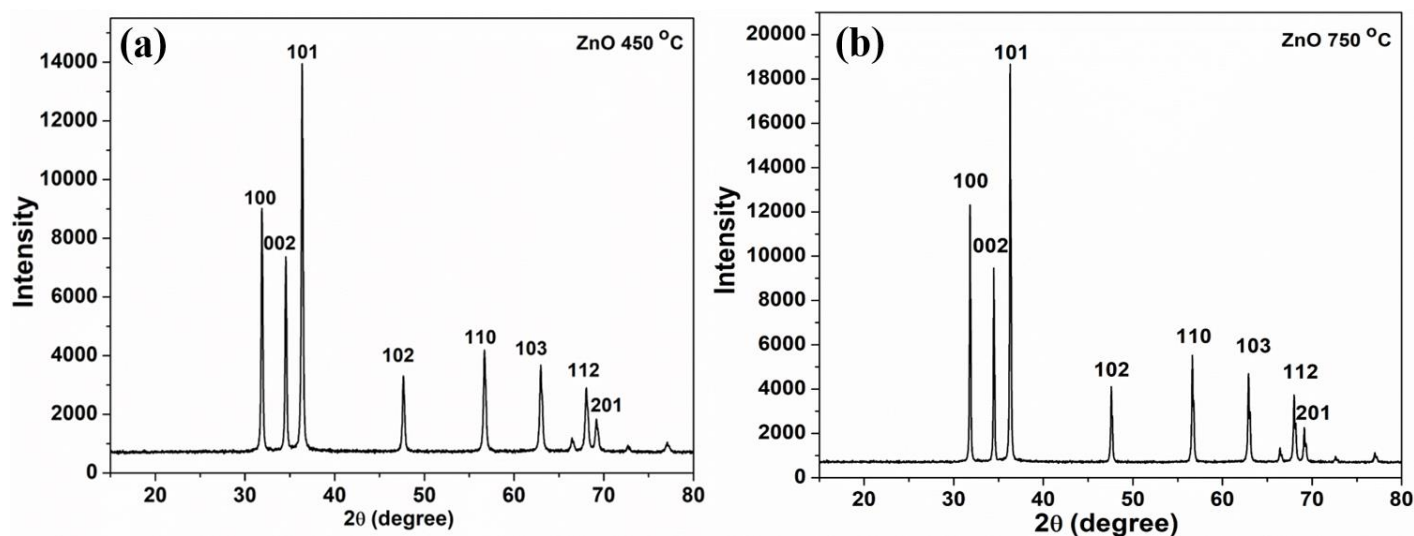


Fig. 2. PXRD pattern of ZnO nanoparticles prepared at (a) 450 °C, and (b) 750 °C.

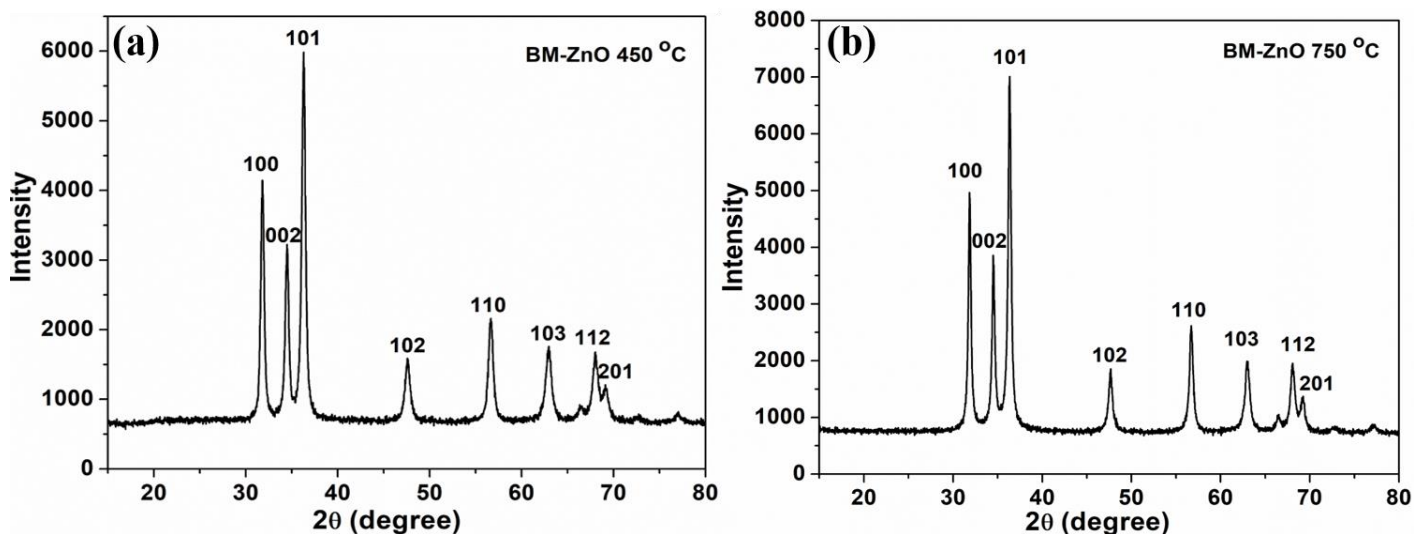


Fig. 3. PXRD pattern of BM-ZnO nanoparticles prepared at (a) 450 °C, and (b) 750 °C.

Table 1. Lattice parameter, Crystallite size, and lattice strain of ZnO and BM- ZnO nanoparticles calcined at 450 °C and 750 °C.

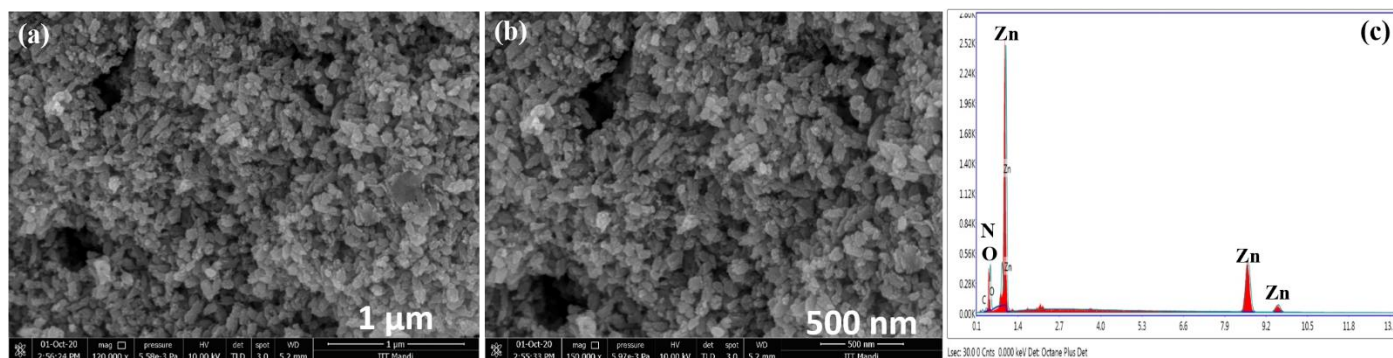
Calcination temperature	2 θ	Lattice constants		Crystallite size	Lattices Strain	Phase	Structure
		a (Å)	c (Å)				
ZnO 450 °C	36.35	2.851	4.939	50	0.0023	Crystalline	Hexagonal wurtzite
ZnO 750 °C	36.29	2.857	4.946	82	0.0014	Crystalline	Hexagonal wurtzite
BM-ZnO 450 °C	36.26	2.862	4.950	18	0.0061	Crystalline	Hexagonal wurtzite
BM-ZnO 750 °C	36.31	2.868	4.952	27	0.0043	Crystalline	Hexagonal wurtzite

Therefore, EDX analysis confirms that sample contains plant as well as Zn and O. The elemental composition of all constituents has been presented in Table 2.

3.3. UV-Visible studies

The UV-visible spectra of bare ZnO NPs at 450 °C, and 750 °C temperatures are depicted in Figure 5. The strong absorption band at about 320 nm and 373 nm confirms the existence of ZnO NPs. However, the observed red shift in

absorption peak with the rise in calcination temperature is the consequence of aggregation of NPs and due to decreased quantum confinement with increasing size [42-46]. The band gap energy (E_g) for synthesized ZnO nanoparticles was evaluated through Tauc plot method. As depicted in Fig, the band gap shows significant increase from 2.78 eV to 2.94 eV due to increment in crystallite size as calcination temperature varies from 450 °C to 750 °C. There is also a slight blue shift in absorption edges with rise in calcination temperature which may be due to the variation in the properties of ZnO NPs [34].

**Fig. 4.** Typical (a) low, and (b) high-magnification SEM images, and (c) EDX spectrum of the prepared BM-ZnO nanoparticles.**Table 2.** Elemental composition of BM- ZnO prepared at 450 °C.

Element	Weight %	Atomic %	Net Int.	K ratio
CK	2.96	9.50	6.25	0.01
NK	2.78	7.64	7.98	0.01
OK	14.98	36.10	141.49	0.05
ZnK	79.28	46.76	511.23	0.74

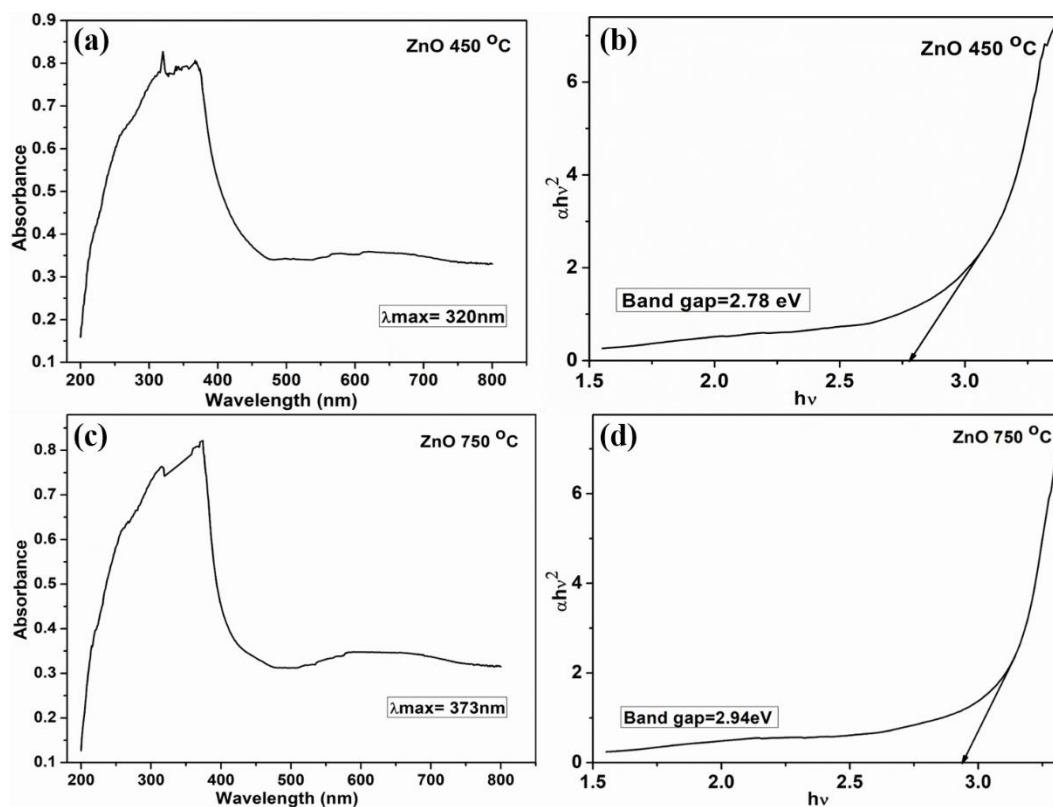


Fig. 5. UV-Visible (a and c) and (b and d) Tauc plot for the synthesized ZnO nanoparticles at 450 °C, and 750 °C, respectively.

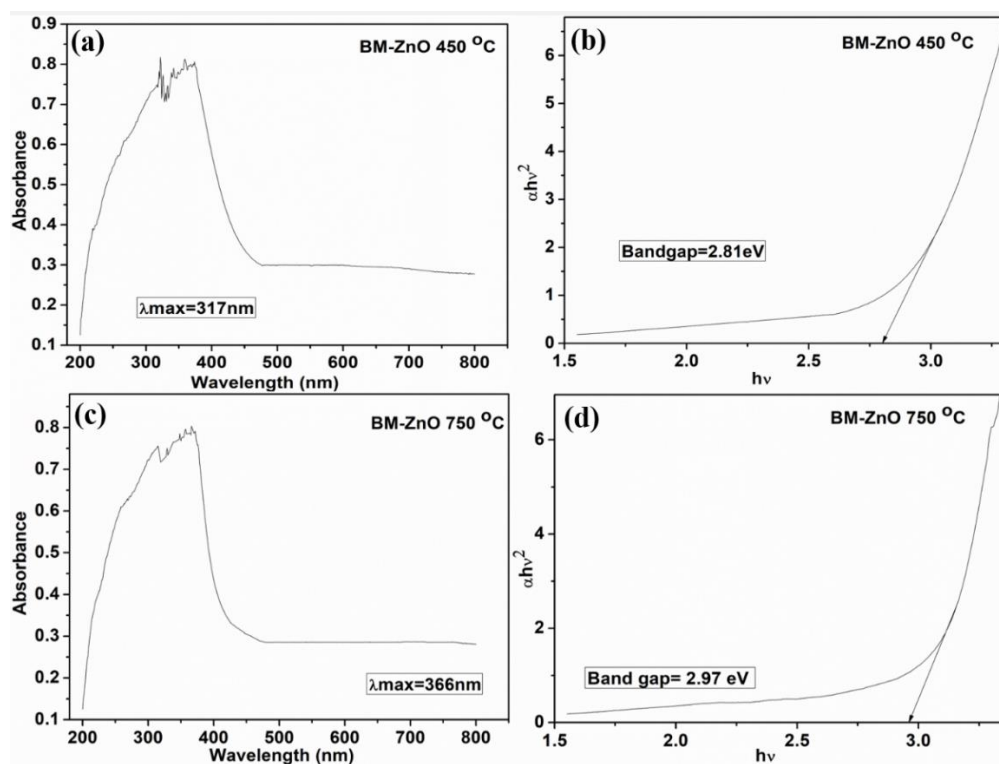


Fig. 6. UV-Visible (a and c) and (b and d) Tauc plot for the synthesized BM-ZnO nanoparticles at 450 °C, and 750 °C, respectively.

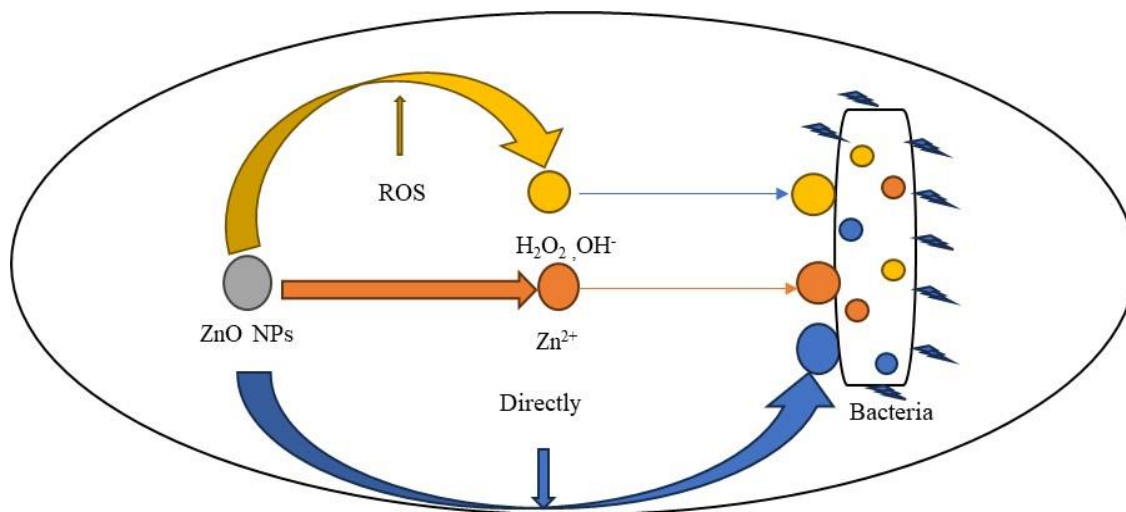


Fig. 7. Mechanism of Antibacterial action of ZnO NPs.

Furthermore, in presence of plant, BM-ZnO NPs exhibit a strong absorption band at about 317 and 366 nm at 450 °C and 750 °C (Figure 6). Band gap energy (E_g) at both temperatures was found to be 2.81 and 2.97 eV. The absorption edges in Figure 6 also tend to shift gradually to a lower wavelength causing blue shift; this is due to the enhancement in the material's crystal quality with rise in calcinated temperature [43].

3.4. Antibacterial Activity Analysis

The in-vitro antibacterial results, summarized in Table 3, highlight the efficacy of both ZnO and BM-ZnO nanoparticles against various bacterial strains. Specifically, ZnO and BM-ZnO exhibited excellent antibacterial activity against Gram-positive bacteria such as *Bacillus cereus*, and *Staphylococcus aureus*, as well as gram-negative bacterium *Stenotrophomonas maltophilia* [44]. However, these nanoparticles demonstrated no inhibitory activity against the Gram-negative bacterium *Shigella flexneri*. Interestingly, biosynthesized BM-ZnO nanoparticles showed a broader spectrum of antibacterial activity, effectively inhibiting almost all tested bacterial strains. This impressive antibacterial activity can be attributed to multiple underlying mechanisms. Primarily, the generation of reactive oxygen species (ROS) such as hydrogen peroxide (H_2O_2) and hydroxyl radicals (OH^\cdot) plays a crucial role. These ROS are highly reactive and can inflict severe oxidative stress on bacterial cells, leading to the degradation of essential cellular components like lipids, proteins, and DNA.

Secondly, the release of zinc ions (Zn^{2+}) from the nanoparticles contributes to their antibacterial effect. Zinc ions can disrupt various metabolic processes within the bacterial cell, impairing enzyme function and protein synthesis [45].

The combined action of ROS formation and zinc ion

release leads to the disruption of the bacterial cell wall and membrane integrity. The oxidative stress induced by ROS compromises the structural stability of the cell wall, making it more permeable and vulnerable to further damage. Simultaneously, the influx of Zn^{2+} ions into the bacterial cell exacerbates the internal stress, disrupting ionic homeostasis and leading to the denaturation of vital biomolecules. These synergistic effects ultimately culminate in the lysis and death of bacterial cells. This dual mechanism of action—ROS generation and Zn^{2+} ion release—makes BM-ZnO nanoparticles highly effective in combating a broad range of bacterial pathogens, including both Gram-positive and Gram-negative strains.

The proposed mechanisms underlying the antibacterial activity of these nanoparticles are illustrated in Figure 7, which depicts the interactions leading to cell wall degradation and subsequent cell death [46].

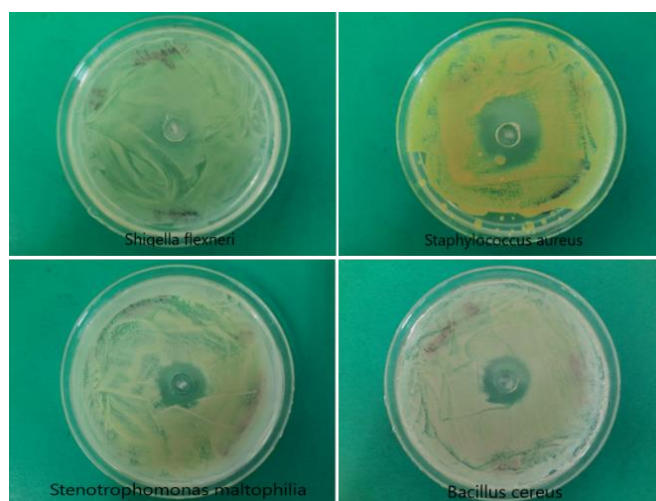


Fig. 8. Antibacterial activity of ZnO at 450 °C against foodborne pathogens shows significant inhibition zones.

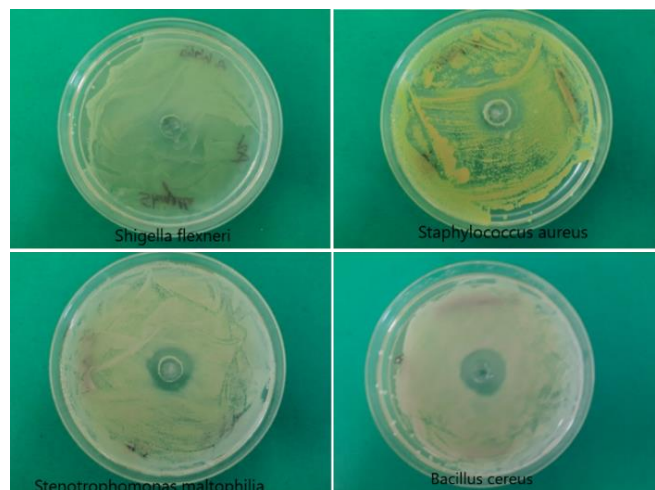


Fig. 9. Antibacterial action of ZnO at 750 °C against foodborne pathogens demonstrates a similar trend of inhibition.

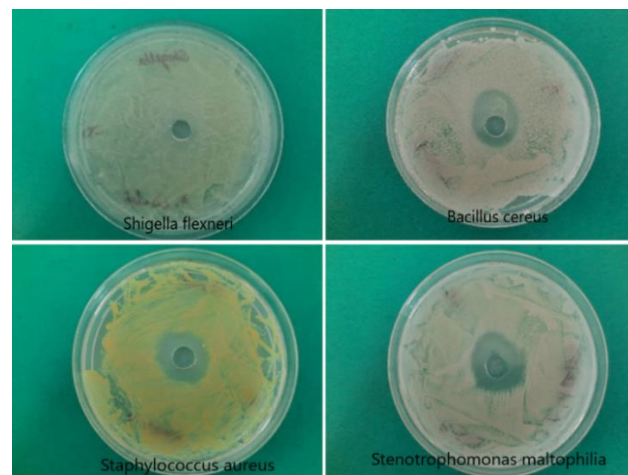


Fig. 10. Antibacterial action of BM-ZnO at 450 °C against foodborne pathogens exhibits enhanced activity compared to bare ZnO.

Table 3. Antibacterial activity of ZnO and BM-ZnO NPs at 450 °C and 750 °C.

Tested compounds	Concentration	The size of inhibition zone (diameter in mm)			
		Gram-negative bacterium		Gram-positive bacterium	
		<i>Stenotrophomonas maltophilia</i> MTCC 4383	<i>Shigella flexneri</i> MTCC 1457	<i>Bacillus cereus</i> MTCC 1272	<i>Staphylococcus aureus</i> MTCC 96
ZnO (450 °C)		5	-	5	10
ZnO (750 °C)		5	-	4	2
BM-ZnO (450 °C)	1 mg ml ⁻¹	6	-	5	7
BM-ZnO (750 °C)		5	-	5	8

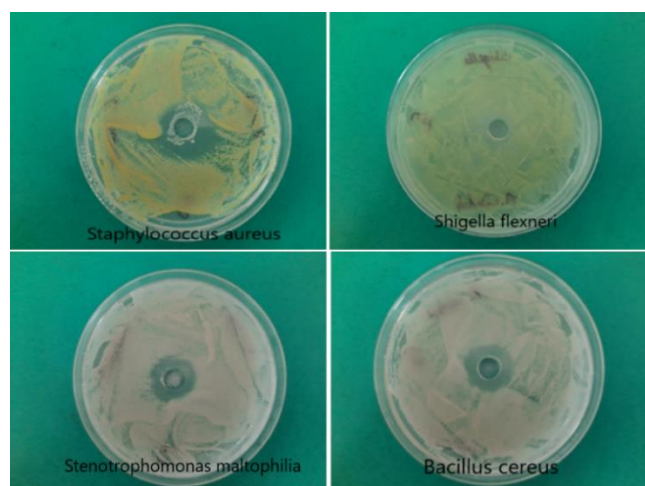


Fig. 11. Antibacterial action of BM-ZnO at 750 °C against foodborne pathogens further underscores the superior efficacy of BM-ZnO nanoparticles.

Figure 8-11 illustrate the zones of inhibition observed for various bacterial strains under different thermal conditions of the nanoparticles. These results suggest that the synthesis method and thermal treatment of ZnO nanoparticles significantly influence their antibacterial properties. Specifically, the biosynthesis of BM-ZnO enhances the nanoparticles' interaction with bacterial cell walls, leading to more effective antibacterial activity. The enhanced performance of BM-ZnO against gram-positive (GP) bacteria indicates its potential for targeted antibacterial applications, especially in environments where GP pathogens are prevalent. This suggests that optimizing the synthesis and thermal treatment of ZnO nanoparticles can tailor their antibacterial properties for specific needs. The insights from these findings can guide the development of more effective antibacterial agents based on ZnO nanoparticles, optimized for specific bacterial targets and environmental conditions. Consequently, this research paves the way for innovative approaches in combating bacterial infections, addressing the growing

concern of antibiotic resistance, and improving public health outcomes.

4. CONCLUSION

This study presented an eco-friendly and straightforward method for synthesizing ZnO nanoparticles using an aqueous extract of *Butea monosperma*. The synthesis process yielded ZnO nanoparticles (NPs) characterized by a hexagonal wurtzite phase, as confirmed by X-ray diffraction (XRD) analysis. The crystallite sizes of the ZnO NPs ranged from 50 to 85 nm at different synthesis temperatures. In contrast, the *Butea monosperma*-mediated ZnO nanoparticles (BM-ZnO NPs) had smaller crystallite sizes, between 15 and 30 nm, indicating the influence of the plant extract on nanoparticle formation. Scanning electron microscopy (SEM) images revealed that the biosynthesized ZnO NPs exhibited both spherical and hexagonal shapes, with sizes ranging from 20 to 90 nm, corroborating the XRD results. Energy-dispersive X-ray (EDX) analysis further confirmed the successful incorporation of ZnO, validating the biosynthesis process. UV-Visible spectroscopy analysis indicated a strong absorption maximum below 400 nm for all nanoparticles, with the optical absorption edge displaying a blue shift as the calcination temperature increased. This blue shift, along with an increase in the bandgap of the ZnO NPs with rising calcination temperatures, is attributed to changes in particle size and the quantum confinement effect.

The antibacterial activity of the biosynthesized ZnO nanoparticles was evaluated against both Gram-positive (GP) and Gram-negative (GN) bacteria. The results showed higher and more effective antibacterial activity against GP bacteria, such as *Staphylococcus aureus* and *Bacillus cereus*, compared to GN bacteria, such as *Stenotrophomonas maltophilia* and *Shigella flexneri*. This enhanced activity is likely due to the interaction of ZnO NPs with the cell walls of GP bacteria, which have a thicker peptidoglycan layer. The plant-mediated synthesis of ZnO nanoparticles using *Butea monosperma* is a promising approach for producing effective antibacterial agents. The biosynthesized ZnO NPs demonstrated strong and promising antibacterial activity, particularly against GP bacteria, suggesting their potential applications in bacterial decontamination and other biological systems. This green synthesis method not only offers an environmentally friendly alternative to conventional chemical synthesis but also enhances the functional properties of ZnO nanoparticles, making them suitable for various biomedical and environmental applications.

CONFLICT OF INTEREST

The authors declare that there is no conflict of interests.

REFERENCES

1. Khan, I., Saeed, K. and Khan, I., **2019**. Nanoparticles: Properties, applications and toxicities. *Arabian Journal of Chemistry*, *12*, pp.908–931.
2. Soni, A., Kumar, M., Sharma, A., Maurya, I.K., Thakur, A. and Kumar, S., **2019**. Synthesis of ultra-small iron oxide and doped iron oxide nanostructures and their antimicrobial activities. *Journal of Taibah University for Science*, *13*, pp.280–285.
3. Gautam, S., Agrawal, H., Thakur, M., Akbari, A., Sharda, H., Kaur, R. and Amini, M., **2020**. Metal oxides and metal organic frameworks for the photocatalytic degradation: A review. *Journal of Environmental Chemical Engineering*, *8*, p.103726.
4. Soni, A., Kaushal, D., Kumar, M., Sharma, A., Maurya, I.K. and Kumar, S., **2022**. Synthesis, characterizations and antifungal activities of copper oxide and differentially doped copper oxide nanostructures. *Materials Today: Proceedings*, <https://doi.org/10.1016/j.matpr.2022.09.133>, in press.
5. Kumar, S., Kumar, M., Thakur, A. and Patial, S., **2017**. Water treatment using photocatalytic and antimicrobial activities of tin oxide nanoparticles. *Indian Journal of Chemical Technology*, *24*, pp.435-440.
6. Jayachandran, A., Aswathy, T.R. and Nair, A.S., **2021**. Green synthesis and characterization of zinc oxide nanoparticles using *Cayratia pedata* leaf extract. *Biochemistry and Biophysics Reports*, *26*, p.100995 (1-8).
7. Pandit, C., Roy, A., Ghotekar, S., Khusro, A., Islam, M.N., Emran, T.B., Lam, S.E., Khandaker, M.U. and Bradley, D.A., **2022**. Biological agents for synthesis of nanoparticles and their applications. *Journal of King Saud University – Science*, *34*, p.101869 (1-13).
8. Dobrucka, R., Długaszewska, J., **2016**. Biosynthesis and antibacterial activity of ZnO nanoparticles using *Trifolium Pratense* flower extract. *Saudi Journal of Biological Sciences*, *23(4)*, pp.517-523.
9. Dadwal, A., Kumari, P., Nike, T., Chauhan, V., Kumar, R., Kaushal, D., Jaswal, V.S., Koundal, A. and Kumar, M., **2024**. Green synthesis of Titanium dioxide nanoparticles by utilizing *Marchantia polymorpha* and their applications in Methylene Blue dye removal. *Catalysis Letters*, <https://doi.org/10.1007/s10562-024-04690-2>. pp.1-14.
10. Nilavukkarasi, M., Vijayakumar, S. and Prathipkumar, S., **2020**. *Capparis zeylanica* mediated bio-synthesized ZnO nanoparticles as antimicrobial, photocatalytic and anti-cancer applications. *Materials Science for Energy Technologies*, *3*, pp.335-343.
11. Romeilah, R., Fayed, S.A. and Mahmoud, G., **2010**. Chemical compositions, antiviral and antioxidant activities of seven essential oils. *Journal of Applied Sciences Research*, *6(1)*, pp.50-62.
12. Naseer, M., Aslam, U., Khalid, B. and Chen, B., **2020**. Green route to synthesize Zinc Oxide Nanoparticles using leaf extracts of *Cassia fistula* and *Melia azadarach*

- and their antibacterial potential. *Scientific Reports* 10 (9055), pp.1-10.
13. Dagdeviren, C., Hwang, S.W., Su, Y., Kim, S., Cheng, H., Gur, O., Haney, R., Omenetto, F.G., Huang, Y. and Rogers, J.A., **2013**. Transient, biocompatible electronics and energy harvesters based on ZnO. *Small*, 9(20), pp.3398-3404.
 14. Meenakshi, Kumar, S., Saralch, S., Dhiman, N., Kumar, M. and Pathak, D., **2018**. Dip Coated ZnO Films for Transparent Window Applications. *Journal of Nano Electronic Physics*, 10(5), p.05038 (1-5).
 15. Kumar, R., Umar, A., Kumar, G. and Nalwa, H.S. **2017**. Antimicrobial Properties of ZnO Nanomaterials: A Review. *Ceramics International*, 43 (5), pp.3940-3961.
 16. Santhoshkumar, J., Kumar, S.V. and Rajeshkumar, S., **2017**. Synthesis of zinc oxide nanoparticles using plant leaf extract against urinary tract infection pathogen. *Resource-Efficient Technologies*, 3(4), pp.459-465.
 17. Faisal, S., Jan, H., Shah, S.A., Khan, A., Akbar, M.T., Rizwan, M., Jan, F., Wajidullah, Akhtar, N., Khatkhat, A. and Syed, S., **2021**. Green Synthesis of Zinc Oxide (ZnO) Nanoparticles Using Aqueous Fruit Extracts of *Myristica fragrans*: Their Characterizations and Biological and Environmental Applications. *ACS Omega*, 6, pp.9709-9722.
 18. Handago, D.T., Zereffa, E.A. and Gonfa, B.A., **2019**. Effects of *Azadirachta indica* leaf extract, capping agents, on the synthesis of pure and Cu doped ZnO-nanoparticles: a green approach and microbial activity. *Open Chemistry*, 17(1), pp.246-253.
 19. Ansari, M.A., Murali, M., Prasad, D., Alzohairy, M.A., Almatroudi, A., Alomary, M.N., Udayashankar, A.C., Singh, S.B., Asiri, S.M.M., Ashwini, B.S. and Gowtham, H.G., **2020**. *Cinnamomum verum* bark extract mediated green synthesis of ZnO nanoparticles and their antibacterial potentiality. *Biomolecules*, 10(2), p.336 (1-15).
 20. Ravindran, C.P., Manokari, M. and Shekhawat, M.S., **2016**. Biogenic production of zinc oxide nanoparticles from aqueous extracts of *Duranta erecta* L. *World Scientific News*, 28, pp.30-40.
 21. Elumalai, K., Velmurugan, S., Ravi, S., Kathiravan, V. and Raj, G.A., **2015**. Bio-approach: Plant mediated synthesis of ZnO nanoparticles and their catalytic reduction of methylene blue and antimicrobial activity. *Advanced Powder Technology*, 26(6), pp.1639-1651.
 22. Ogunyemi, S.O., Abdallah, Y., Zhang, M., Fouad, H., Hong, X., Ibrahim, E., Masum, M.M.I., Hossain, A., Mo, J. and Li, B., **2019**. Green synthesis of zinc oxide nanoparticles using different plant extracts and their antibacterial activity against *Xanthomonas oryzae* pv. *Oryzae*. *Artificial Cells Nanomedicine and Biotechnology*, 47(1), pp.341-352.
 23. Gunalan, S., Sivaraj, R. and Rajendran, V., **2012**. Green synthesized ZnO nanoparticles against bacterial and fungal pathogens. *Progress in Natural Science: Materials International*, 22(6), pp.693-700.
 24. Kaushik, M., Niranjana, R., Thangam, R., Madhan, B., Pandiyarasan, V., Ramachandran, C., Oh, D.H. and Venkatasubbu, G.D., **2019**. Investigations on the antimicrobial activity and wound healing potential of ZnO nanoparticles. *Applied Surface Science*, 479, pp.1169-1177.
 25. Navale, G.R., Thripuranthaka, M., Dattatray, J.L. and Shinde, S.S., **2015**. Antimicrobial Activity of ZnO Nanoparticles against Pathogenic Bacteria and Fungi. *JSM Nanotechnology and Nanomedicine* 3(1), p.1033 (1-9).
 26. Isik, T., Hilal, M.E. and Horzum, N., Ed. **2019**. Green synthesis of zinc oxide nanostructures. In: *Zinc Oxide Based Nano Materials and Devices*, Intech Open, pp.1-28.
 27. Kadiyala, U., Turali-Emre, E.S., Bahng, J.H., Kotov, N.A. and VanEpps, J.S., **2018**. Unexpected insights into antibacterial activity of zinc oxide nanoparticles against methicillin resistant *Staphylococcus aureus* (MRSA). *Nanoscale*, 10, pp.4927-4939.
 28. Kumari, P., Raina, K., Thakur, S., Sharma, R., C-Martins, N., Kumar, P., Barman, K., Sharma, S., Kumar, D., Prajapati, P. K., Sharma, R. and Chaudhary, A., **2022**. Ethnobotany, Phytochemistry and Pharmacology of Palash (*Butea monosperma* (Lam.) Taub.): a Systematic Review. *Current Pharmacology Reports*, 8, pp.188-204.
 29. Moore, D.M. and Reynolds, R.C. Jr., 2nd Ed. **1997**. *X-Ray diffraction and the identification and analysis of clay minerals*, Oxford University Press, New York.
 30. Rashmi, B.N., Harlapur, S.F., Avinash, B., Ravikumar, C.R., Nagaswarupa, H.P., Kumar, M.R.A., Gurushantha, K. and Santosh, M.S., **2020**. Facile green synthesis of silver oxide nanoparticles and their electrochemical, photocatalytic and biological studies. *Inorganic Chemistry Communications*, 111, p.107580.
 31. Cullity, B.D., Ed. **1967**. *Elements of X-ray Diffraction*, Adison-Wesley Publ. Co., London.
 32. Srivastava, V., Gusain, D. and Sharma, Y.C., **2013**. Synthesis, characterization and application of zinc oxide nanoparticles (n-ZnO). *Ceramics International*, 39 (8), pp.9803-9808.
 33. Ghamsari, M.S., Alamdari, S., Razzaghi, D. and Pirlar, M.A., **2019**. ZnO nanocrystals with narrow-band blue emission. *Journal of Luminescence*, 205, pp.508-518.
 34. Kayani, Z.N., Saleemi, F. and Batool, I., **2015**. Effect of calcination temperature on the properties of ZnO nanoparticles. *Applied Physics A, Material Science Process*, 119, pp.713-720.
 35. Ashraf, R., Riaz, S., Kayani, Z.N. and Naseem, S., **2015**. Effect of Calcination on properties of ZnO nanoparticles. *Materials Today: Proceedings*, 2, pp.5468-5472.
 36. Kumar, S.S., Venkateswarlu, P., Rao, V.R. and Rao, G.N., **2013**. Synthesis, characterization and optical properties of zinc oxide nanoparticles. *International Nano Letters*, 3, p.30 (1-6).
 37. Suresh, J., Pradheesh, G., Alexramani, V., Sundrarajan, M. and Hong, S.I., **2018**. Green synthesis and

- characterization of zinc oxide nanoparticle using insulin plant (*Costus pictus D. Don*) and investigation of its antimicrobial as well as anticancer activities. *Advances in Natural Sciences: Nanoscience and Nanotechnology*, 9, p.015008 (1-8).
38. Darroudi, M., Sabouri, Z., Oskuee, R.K., Zak, A.K., Kargar, H. and Hamid, M.H.N.A., **2014** Green chemistry approach for the synthesis of ZnO nanopowders and their cytotoxic effects. *Ceramics International*, 40, pp.4827-4831.
39. Ashokraja, C., Sakar, M. and Balakumar, S., **2017**. A perspective on the hemolytic activity of chemical and green-synthesized silver and silver oxide nanoparticles. *Materials Research Express*, 4, p.105406 (1-12).
40. Singh, R.P.P., Hudiara, I.S. and Rana, S.B., **2016**. Effect of calcination temperature on the structural, optical and magnetic properties of pure and Fe-doped ZnO nanoparticles. *Materials Science-Poland*, 34, pp.451-459.
41. Ali, S.G., Ansari, M.A., Jamal, Q.M.S., Almatroudi, A., Alzohairy, M.A., Alomary, M.N., Rehman, S., Mahadevamurthy, M., Jalal, M., Khan, H.M., Adil, S.F., Khan, M. and Al-Warthan, A., **2021**. *Butea monosperma* seed extract mediated biosynthesis of ZnO NPs and their antibacterial, antibiofilm and anti-quorum sensing potentialities. *Arabian Journal of Chemistry*, 14, p.103044 (1-11).
42. Getie, S., Belay, A., Chandra Reddy, A.R. and Belay, Z., **2017**. Synthesis and characterizations of zinc oxide nanoparticles for antibacterial applications. *Journal of Nanomedicine Nanotechnology*, 88, pp.1-8.
43. Alibe, I.M., Matori, K.A., Saion, E., Ali, A.M. and Zaid, M.H.M., **2017**. The influence of calcination temperature on structural and optical properties of ZnO nanoparticles via simple polymer synthesis route. *Science of Sintering*, 49, pp.263-275.
44. Klink, M.J., Laloo, N., Taka, A.L., Pakade, V.E., Monapathi, M.E. and Modise, J.S., **2022** Synthesis, Characterization and Antimicrobial Activity of Zinc Oxide Nanoparticles against Selected Waterborne Bacterial and Yeast Pathogens. *Molecules*, 27, p.3532 (1-13).
45. Vimbela, G.V., Ngo, S.M., Frazee, C., Yang, L. and Stout, D.A., **2017**. Antibacterial properties and toxicity from metallic nanomaterials. *International Journal of nanomedicine*, 12, pp.3941-3965.
46. Tayel, A.A., El-Tras, W.F., Moussa, S., El-Baz, A.F., Mahrous, H., Salem, M.F. and Brimer, L., **2011**. Antibacterial action of zinc oxide nanoparticles against foodborne pathogens. *Journal of Food Safety*, 31, pp.211-218.